Detection of a Noble Gas Molecular Ion, $^{36}ArH^{+}$, in the Crab Nebula

M. J. Barlow[1†], B. M. Swinyard[1,2], P. J. Owen[1], J. Cernicharo[3], H. L. Gomez[4], R. J. Ivison[5], O. Krause[6], T. L. Lim[2], M. Matsuura[1], S. Miller[1], G. Olofsson[7], E. T. Polehampton[2,8]

[1]Dept. of Physics & Astronomy, University College London, Gower Street, London WC1E 6BT, UK

[2]Space Science & Technology Department, Rutherford Appleton Laboratory, Didcot OX11 0QX, UK

[3]Laboratory of Molecular Astrophysics, Dept. of Astrophysics, CAB, INTA-CSIC, Ctra de Ajalvir, km 4, 28850 Torrejón de Ardoz, Madrid, Spain

[4]School of Physics & Astronomy, Cardiff University, The Parade, Cardiff CF24 3AA, UK

[5]UK Astronomy Technology Centre, Royal Observatory Edinburgh, Blackford Hill, Edinburgh EH9 3HJ, UK

[6]Max-Planck-Institut für Astronomie, Königstuhl 17, D-69117 Heidelberg, Germany

[7]Dept. of Astronomy, Stockholm University, AlbaNova University Center, Roslagstulsbacken 21, 10691 Stockholm, Sweden

[8]Institute for Space Imaging Science, Dept. of Physics & Astronomy, University of Lethbridge, Lethbridge, Alberta T1K 3M4, Canada

[†]email:mjb@star.ucl.ac.uk; Published in Science, v.342, pp.1343-1345, 2013

Noble gas molecules have not hitherto been detected in space. From spectra obtained with the *Herschel Space Observatory*, we report the detection of emission in the 617.5 GHz and 1234.6 GHz J = 1-0 and 2-1 rotational lines of $^{36}ArH^{+}$ at several positions in the Crab Nebula, a supernova remnant known to contain both H_2 molecules and regions of enhanced ionized argon emission. ^{36}Ar is believed to have originated from explosive nucleosynthesis in massive

stars during core-collapse supernova events. Its detection in the Crab Nebula, the product of such a supernova event, confirms this expectation. The likely excitation mechanism for the observed ^{36}ArH$^+$ emission lines is electron collisions in partially ionized regions with electron densities of a few hundred per centimeter cubed.

Noble gas compounds have not yet been found in space, despite some examples, such as ionized hydrides, being relatively stable (1). Astronomical searches for the near-infrared and far-infrared lines of HeH$^+$, whose dissociation energy is 1.8 eV (2) have not been successful (3, 4). The Crab Nebula is the product of the supernova of 1054 AD and is thought to have originated from the core-collapse explosion of a star 8-16 times as massive as the Sun (5). We have obtained far-infrared to submillimeter spectra of the Crab Nebula using the *Herschel Space Observatory* (6). We report here the detection of emission lines from the ionized hydride of argon, an element predicted to form by explosive nucleosynthesis in core-collapse supernovae (7).

The Crab Nebula was observed with the Fourier Transform Spectrometer (FTS) of the Spectral and Photometric Imaging Receiver (SPIRE) (8, 9) on Operational Day 466 of the *Herschel* mission, as part of the Mass-loss of Evolved StarS (MESS) Guaranteed Time Key Project (10). The 19 SPIRE Long Wavelength (SLW) detectors, each with a beamwidth of $\sim$37$''$, covered the 447-989 GHz frequency range (303-671 μm), while 35 SPIRE Short Wavelength (SSW) detectors, each with a beamwidth of $\sim$18$''$, covered the 959-1544 GHz frequency range (194-313 μm) (Fig. 1). The full width half maximum spectral resolution was 1.44 GHz at all frequencies, corresponding to a resolving power of 690 in the middle of the frequency range. The observation consisted of 48 FTS scans, for a total on-source exposure time of 3197s. The data were processed using the extended source calibration in version 11 of the Herschel Interactive Processing Environment (11). The J = 2-1, F = 5/2-3/2 line of OH$^+$ at 971.8038 GHz (12), which falls in the SLW and SSW spectral overlap region, is present in emission in many of the spectra (Fig. 2). This line has been observed from a range of astrophysical environments by *Herschel*, both in absorption (13) and emission (14, 15). In addition, two unidentified emission lines were found to be present in some of the Crab spectra, one in the SLW range at $\sim$618 GHz, and the other in the SSW range at $\sim$1235 GHz.

The knots and filaments of the Crab Nebula are known to exhibit expansion velocities ranging between 700-1800 km s^{-1} (16); in different detectors we measured radial velocities for the OH^+ 971.8038 GHz line that ranged between -603 and +1037 km s^{-1}. Several spectra showed multiple OH^+ velocity components, some blended, but in most spectra the OH^+ velocity components were unresolved, exhibiting very different radial velocities from detector to detector, consistent with an origin from differing knots or filaments in the nebula, each with its own discrete velocity. Because OH^+ was the only identified species in the spectra initially, we used the measured radial velocities of the 971.8038 GHz OH^+ line, whose centroid frequency could typically be measured to an accuracy of $\pm$(25-40) km s^{-1}, as a reference to correct to a 'rest' frequency the observed frequencies of the 618 or 1235 GHz line falling in the same spectrum. There were four SLW spectra, those from detectors B3, C3, D3 and D4, in which the OH^+ line and the 618 GHz line were both present, with emission line surface brightnesses in excess of 2×10^{-10} W m^{-2} sr^{-1}. These four spectra yielded a mean 'rest' frequency for the 618 GHz line of 617.554 $\pm$ 0.209 GHz. The 1235 GHz line was detected in five SSW spectra (A2, B1, B2, B3 and D4) but only in the B1 (Fig. 2) and B3 spectra were both it and the 971.8038 GHz OH^+ line present with a single unresolved component. The J = 1-1, F = 1/2-1/2 line of OH^+ at 1032.998 GHz was also detected in emission in the SSW B1 spectrum, enabling a third estimate of the rest frequency of the 1235 GHz line. The mean frequency derived from these three estimates was 1234.786 $\pm$ 0.643 GHz.

The ratio of the derived rest frequencies of 1234.786 $\pm$ 0.643 GHz and 617.554 $\pm$ 0.209 GHz is 1.9995$\pm$0.0012, which suggests that the lines correspond to the 2-1 and 1-0 rotational transitions of a simple diatomic molecule (we can rule out their being 4-3 and 2-1 transitions, with a frequency ratio of 4:2, because of the lack of a corresponding 3-2 transition at $\sim$ 926 GHz). A search using the *Cologne Database for Molecular Spectroscopy* (12) and the MADEX code (17) found the only candidate to be ^{36}ArH$^+$, whose 1-0 and 2-1 rotational transitions lie at 617.52523 $\pm$ 0.00015 GHz and 1234.60275 $\pm$ 0.00030 GHz, respectively, agreeing with the derived frequencies for the Crab Nebula lines within the uncertainties. The 1-0 and 2-1 rotational transitions of ^{40}ArH$^+$ are at 615.85813 $\pm$ 0.00005 GHz and 1231.27100 $\pm$ 0.00009 GHz, while the corresponding transitions of ^{38}ArH$^+$ are at 616.64871 $\pm$ 0.00004 GHz and 1232.85100 $\pm$ 0.00004 GHz, ruling out these two isotopic variants as identifications. Argon is the third most abundant species in the Earth's atmosphere, 0.93% by number, with ^{40}Ar/^{38}Ar/^{36}Ar isotopic ratios of to 1584/1.00/5.30 (18). However, ^{40}Ar in the earth's atmosphere is a product of the decay, mainly in rocks, of ^{40}K, whose half-life is 1.25$\times$10^9 yrs. For the solar wind the ^{40}Ar/^{38}Ar/^{36}Ar isotopic ratios have been measured to be 0.00/1.00/5.50 (19). ^{36}Ar is expected to be the dominant isotope of argon in stars, being an explosive nucleosynthesis product of the α-particle capture chain that takes place in massive star core-collapse supernovae (7). Regions of enhanced emission from optical forbidden lines of ionized argon have previously been mapped in the Crab Nebula by a number of authors (20–22), almost certainly corresponding to enriched argon abundances. Strongly enhanced infrared forbidden lines of Ar$^+$ and Ar^{2+} have been detected from the southern filament (22) where we find ^{36}ArH$^+$ line emission to be strongest (SSW detector B1; Fig. 1 and Table 1). The enhanced lines of ionized argon and ^{36}ArH$^+$ strongly indicate the presence there of pockets of ^{36}Ar produced by explosive nucleosynthesis during the supernova event.

The ^{38}Ar isotope of argon is also predicted to be synthesised in core-collapse supernova events (7). We used Crab Nebula SPIRE-FTS spectra in which the ^{36}ArH$^+$ velocity components are strong and narrow to put limits on the isotopic ratios of ^{40}Ar and ^{38}Ar relative to ^{36}Ar in the emitting regions. Because the frequency separation between the isotopic variants of ArH^+ is a factor of two larger for the J = 2-1 lines than for the 1-0 lines, whereas the SPIRE-FTS frequency resolution is constant, the 2-1 lines are better suited for placing limits on the isotopic ratios of argon. Relative to the $^{36}ArH^+$ 2-1 line, the separation of the $^{40}ArH^+$ 2-1 line is -3.33175 GHz, while that of the $^{38}ArH^+$ 2-1 line is -1.75175 GHz. To estimate upper limits to the abundances of these species, we added synthetic lines to the spectra having the appropriate frequency offset and the same line width as the $^{36}ArH^+$ 2-1 line, changing the strength of the synthetic lines until the signal-to-noise ratio estimated by the line-fitting routine reached 3σ. The SSW B1 (Fig. 2) and SSW B3 spectra both yielded 3σ lower limits to the abundance ratio of $^{36}ArH^+$/$^{38}ArH^+$ of > 2, along with $^{36}ArH^+$/$^{40}ArH^+$ lower limits of > 5 and > 4, respectively.

ArH^+ is a stable molecular ion (dissociation energy D_0 = 3.9$\pm$0.1 eV (1)) that has been studied extensively in the laboratory. The Crab Nebula consists predominantly of ionized gas, photoionized by synchrotron radiation from the pulsar wind nebula (5, 16). It also contains many H_2-emitting neutral clumps (23, 24). Transition zones between fully ionized and molecular gas will exist, where ArH^+ can be formed by the exothermic reaction $Ar^+ + H_2 \rightarrow ArH^+ + H$, releasing 1.49 eV (25). If the elemental species created by the supernova explosion were still largely unmixed in the remnant, then it is possible that ArH^+ molecules would be found only at interfaces between H-rich gas and Ar-rich gas where mixing has occurred. Four of the seven FTS SSW detectors in whose spectra J = 2-1 $^{36}ArH^+$ emission was detected (SSW B1, B2, A1 and A2) are situated on a bright filament south of the center of the nebula (Fig. 1), as is the SLW D4 detector in which the strongest J = 1-0 emission was detected. A cluster of seven near-infrared H_2-emitting knots, with a wide range of radial velocities, is coincident with the same bright filament (24). Detectors SLW C3/SSW D4 also show $^{36}ArH^+$ emission and are coincident with an H_2-emitting knot. The lack of ArH^+ emission in the NW quadrant of the nebula is mirrored by a relative lack of H_2 emission knots in that region. However, there are many H_2 knots in the NE quadrant, whereas ArH^+ emission is only detected there in two FTS detectors (SLW E1 and E2).

The reaction rate for the formation of ArH^+ via $Ar^+ + H_2 \rightarrow ArH^+ + H$ is 8.9×10^{-10} cm^3 s^{-1} at 300 K (25). Reaction rates are known for the ArH^+ destruction reaction with H_2 (to yield Ar + H_3^+, with a reaction rate of 6.3×10^{-10} cm^3 s^{-1} at 300 K (26)) and for its dissociative recombination with electrons (ArH^+ + e^- $\rightarrow$ Ar + H^*, with a rate $\leq 5 \times 10^{-10}$ cm^3 s^{-1} at low electron energies (27)). However, because the Crab nebula is photoionized by its pulsar wind nebula (5, 16), photodissociation could be the main ArH^+ destruction mechanism.

The main excitation mechanism for the observed ArH^+ emission lines is likely to be collisions with either electrons or H_2 molecules but rate calculations or measurements do not exist as yet. The J = 1 and 2 levels of $^{36}ArH^+$ are situated 29.6 K and 88.9 K above the ground state, respectively, negligible compared to the electron temperatures of 7500-15000 K measured for the ionized gas in the Crab Nebula (5), or even compared to the H_2 excitation temperatures of 2000-3000 K that have been measured (28). If the electron or H_2 densities in the transition zones where ArH^+ is hypothesised to be located should exceed the 'critical densities' of the emitting levels (where the sum of the collisional excitation and de-excitation rates from a level exceed the radiative decay rate from the level), then the level populations will be in Boltzmann equilibrium. Using the known molecular parameters of ArH^+ (12, 17) the 2-1/1-0 line emission ratios should then be of the order 30, for excitation temperatures appreciably exceeding 100 K. The SSW D4 and SLW C3 detectors are centred on the same bright knot (Fig. 1) and yield a 2-1/1-0 line surface brightness ratio of 2.5, while the spectra from the approximately co-located SSW B3 and SLW C4 detectors yield a line surface brightness ratio of 2.0 (Table 1), well below the ratio for Boltzmann equilibrium. The densities of the collision partners in the emitting regions must therefore be well below the corresponding critical densities of the ArH^+

rotational levels. We used the MADEX code (17) with the molecular parameters of ArH^+, together with SiH^+ + He collisional de-excitation rates (29) in place of those of ArH^+ + H_2, and CH^+ + e^- collisional de-excitation rates (30) in place of those for ArH^+ + e^- (with upward rates calculated using detailed balance and the correct values of the energies for the levels of ArH^+) in order to estimate corresponding H_2 and electron critical densities of $\sim 10^8$ cm^{-3} and $\sim 10^4$ cm^{-3}, respectively. The observed 2-1/1-0 line ratios of 2.5 and 2.0 indicate H_2 densities of a few$\times 10^6$ cm^{-3}, or electron densities of a few$\times 10^2$ cm^{-3}. The calculations take into account opacity effects although the line centre optical depths are estimated to be significantly less than unity for line widths larger than 1 km s^{-1}. For H_2 collisions at temperatures between 100 K and 3000 K and densities of $\sim 10^6$ cm^{-3}, or electron collisions at temperatures of ~3000 K and densities of a few$\times 10^2$ cm^{-3}, we estimate ^{36}ArH$^+$ column densities of $10^{12} - 10^{13}$ cm^{-2}.

Given that likely electron collisional excitation rates are $\sim 10^4$ larger than those of H_2 and that the parent Ar^+ ion must exist in a region that is at least partially ionized, electron collisions are expected to dominate the excitation of ArH^+. A density of $\sim 10^4$ cm^{-3} has been estimated for the Crab H_2 knots (28), a factor of 100 below that required for H_2 collisions to be the excitation mechanism for the ArH^+ lines. This lends further support to electron collisions in partially ionized transition regions being the main ArH^+ excitation mechanism.

Our detection of ^{36}ArH$^+$ in the Crab Nebula suggests that an unidentified multi-component broad absorption feature seen between 617 and 618 GHz in a Herschel HIFI spectrum of Sgr B2(M) (towards the center of our galaxy) (31) can potentially be identified with ground-state absorption in the J = 0-1 617.525 GHz line of ^{36}ArH$^+$ along the interstellar sightline.

References and Notes

1. J. R. Wyatt *et al.*, *J. Chem. Phys.* **62**, 2555 (1975).

2. S. G. Lias, J. F. Liebman, R. D. Levin, *J. Phys. Chem. Ref. Data* **13**, 695 (1984).

3. J. M. Moorhead, R. P. Lowe, W. H. Wehlau, J.-P. Maillard, P. F. Bernath, *Astrophys. J.* **326**, 899 (1988).

4. X.-W. Liu *et al.*, *Mon. Not. R. Astron. Soc.* **290**, L71 (1997).

5. K. Davidson, R. A. Fesen, *Annu. Rev. Astron. Astrophys.* **23**, 119 (1985).

6. G. L. Pilbratt *et al.*, *Astron. Astrophys.* **518**, L1 (2010).

7. D. Arnett, *Supernovae and Nucleosynthesis*, (Princeton Univ. Press, 1996).

8. M. J. Griffin *et al.*, *Astron. Astrophys.* **518**, L3 (2010).

9. B. M. Swinyard *et al.*, *Astron. Astrophys.* **518**, L4 (2010).

10. M. Groenewegen *et al.*, *Astron. Astrophys.* **526**, A162 (2011).

11. S. Ott, *Astr. Soc. Pacific Conf. Ser.* **434**, 139 (2010).

12. H. S. P. Müller, F. Schlöder, J. Stutzki, G. Winnewisser, *J. Mol. Struct.* **742**, 215 (2005).

13. D. A. Neufeld *et al.*, *Astron. Astrophys.* **521**, L10 (2010).

14. P. P. van der Werf *et al.*, *Astron. Astrophys.* **518**, L42 (2010).

15. L. Spinoglio *et al.*, *Astrophys. J.* **758**, 108 (2012).

16. J. J. Hester, *Annu. Rev. Astron. Astrophys.* **46**, 127 (2008).

17. J. Cernicharo, *EAS Publ. Ser.* **58** 251 (2012).

18. J.-Y. Lee *et al.*, *Geochim. et Cosmochim. Acta* **70**, 4507 (2006).

19. A. Meshik *et al.*, *Science* **318**, 433 (2007).

20. G. M. MacAlpine *et al.*, *Astrophys. J.* **432**, L131 (1994).

21. E. L. Schaller & R. A. Fesen, *Astron J.* **123**, 941 (2002).

22. T. Temim *et al.*, *Astrophys. J.* **753**, 72 (2012).

23. J. R. Graham, G. S. Wright, A. J. Longmore, *Astrophys. J.* **352**, 172 (1990).

24. E. F. Loh *et al.*, *Astrophys. J. Suppl. Ser.* **194**, 30 (2011).

25. A. C. Roach, P. J. Kuntz, *Chem. Comms.* 1336 (1970).

26. V. G. Anicich, *NASA JPL Publ.* 03-19 (2003).

27. J. B. A. Mitchell *et al.*, *J. Phys. B* **38**, L175 (2005).

28. E. D. Loh *et al.*, *Mon. Not. R. Astron. Soc.* **421**, 789 (2012).

29. C. Nkem *et al.*, *J. Mol. Struct.* THEOCHEM **901**, 220 (2009).

30. A. J. Lim, I. Rabadán, J. Tennyson, *Mon. Not. R. Astron. Soc.* **306**, 473 (1999).

31. P. Schilke, HEXOS Team, in *Proceedings of the Herschel First Results Symposium*, (2010).
\protect\vrule width0pt\protect\href{http://herschel.esac.esa.int/FirstResultsSymposium/presentations/A34_Schi

32. H. L. Gomez *et al.*, *Astrophys. J.* **760**, 96 (2012).

33. We thank the anonymous referees for their constructive reports. We thank Dr Edwin Bergin for drawing our attention to the 2010 HEXOS Herschel HIFI spectrum of SgR B2(M) that shows an unidentified broad absorption feature below 618 GHz. *Herschel* is an ESA space

observatory with science instruments provided by European-led Principal Investigator consortia and with important participation from NASA. SPIRE has been developed by a consortium of institutes led by Cardiff University (UK) and including Univ. Lethbridge (Canada); NAOC (China); CEA, LAM (France); IFSI, Univ. Padua (Italy); IAC (Spain); Stockholm Observatory (Sweden); Imperial College London, RAL, UCL-MSSL, UKATC, Univ. Sussex (UK); and Caltech, JPL, NHSC, Univ. Colorado (USA). This development has been supported by national funding agencies: CSA (Canada); NAOC (China); CEA, CNES, CNRS (France); ASI (Italy); MINECO (Spain); SNSB (Sweden); STFC and UKSA (UK); and NASA (USA). JC thanks MINECO for financial support under projects AYA2009-07304, AYA2012-32032 and Consolider program ASTROMOL CSD2009-00038.

Table 1: SPIRE-FTS radial velocity and line surface brightness measurements for the J = 1-0 and 2-1 rotational lines of $^{36}ArH^{+}$ from the Crab Nebula

	J = 1-0 617.525 GHz			J = 2-1 1234.603 GHz	
SLW Detector	Radial Velocity km s^{-1}	Surface Brightness 10^{-10} W m^{-2} sr^{-1}	SSW Detector	Radial Velocity km s^{-1}	Surface Brightness 10^{-10} W m^{-2} sr^{-1}
B3	+317 ± 67	2.23 ± 0.41	C5	-1354 ± 26	8.2 ± 1.2
C3	+933 ± 33	4.63 ± 0.40	D4	+743 ± 26	11.7 ± 1.6
C4	-58 ± 50	8.65 ± 0.55	B3	-101 ± 20	17.5 ± 1.4
D3	+826 ± 32	3.13 ± 0.34			
D3	-709 ± 42	2.30 ± 0.34			
D4	+101 ± 27	9.89 ± 0.52	A1	-51 ± 52	13.9 ± 2.0
			B2	-572 ± 25	10.8 ± 1.7
			B1	+140 ± 34	38.4 ± 1.6
			A2	+61 ± 28	10.1 ± 1.4
E1	+278 ± 46	5.69 ± 0.62			
E2	-594 ± 37	4.25 ± 0.46			

Fig. 1. A broad-band Herschel-PACS image mapping the 70-μm dust emission from the Crab Nebula. North is up and East is to the left. The positions on the nebula of the 19 SLW and 35 SSW detectors of the SPIRE FTS are marked with circles whose angular diameters of 37$''$ and 18$''$ correspond to the SLW and SSW beam sizes. The positions of detectors in whose spectra the J = 1-0 or 2-1 rotational lines of ^{36}ArH^{+} were detected are marked with crosses.

Fig. 2. SPIRE FTS spectra of the Crab Nebula, plotting surface brightness in W m^{-2} Hz^{-1} sr^{-1} against frequency in GHz. Several emission lines are superposed on a continuum attributed to thermal dust emission (32). Upper plot: the spectrum from the SLW D4 detector, whose position on the nebula is marked in Fig. 1. Emission line velocity components attributed to the J = 2-1, F = 5/2-3/2 971.8038 GHz rotational line of OH^{+} and the J = 1-0 617.525 GHz rotational line of ^{36}ArH^{+} are visible. Lower plot: the SSW B1 spectrum. In addition to OH^{+} 971.8038 GHz velocity components, emission in the J = 2-1 1234.603 GHz line of ^{36}ArH^{+} is visible. The radial velocities and surface brightnesses of the ^{36}ArH^{+} emission lines that are present in the spectra obtained from these and other FTS detectors are listed in Table 1.

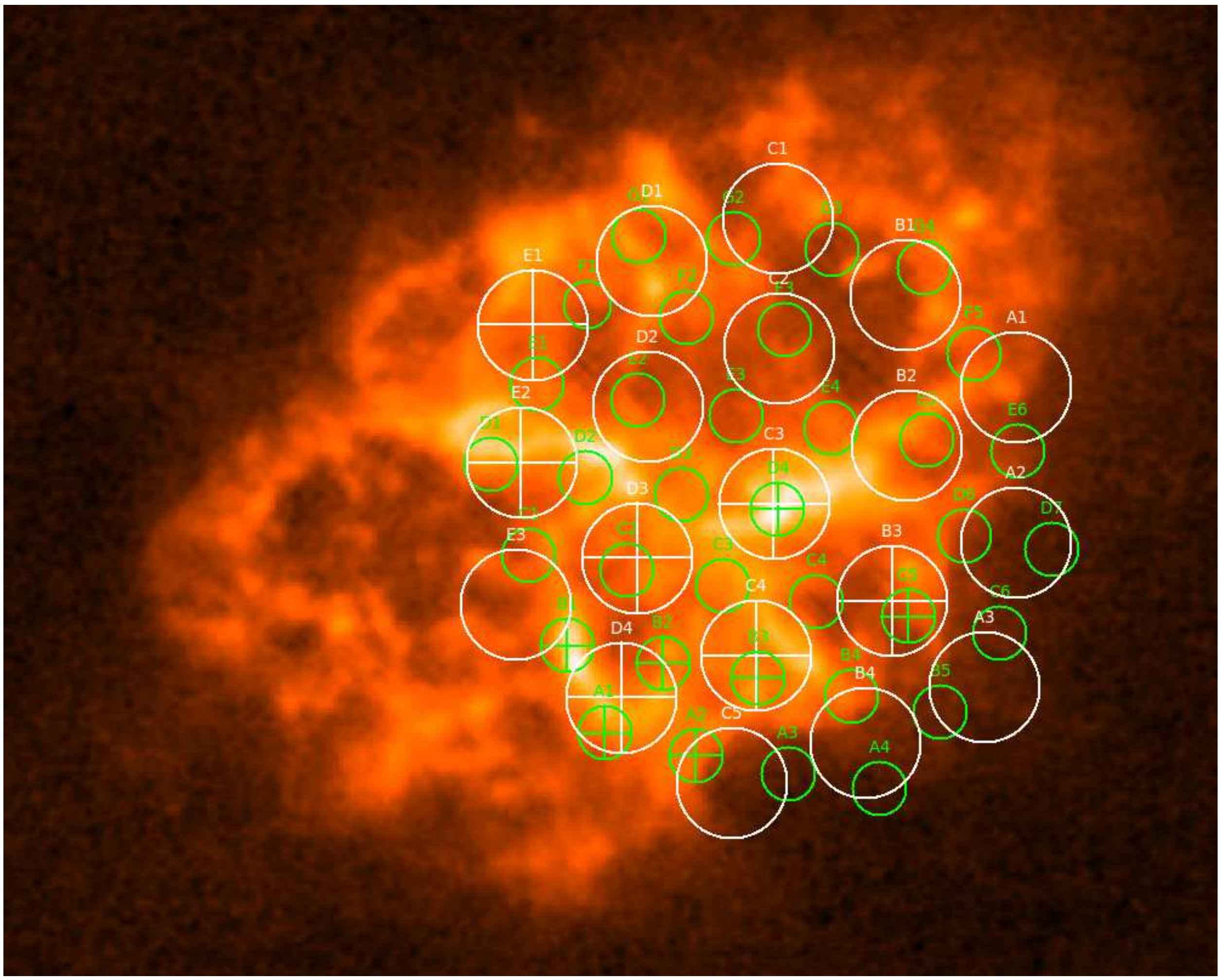
C1
D1
B1
E1
C2
A1
D2
B2
E2
C3
A2
D3
B3
E3
C4
D4
A3
B4
C5

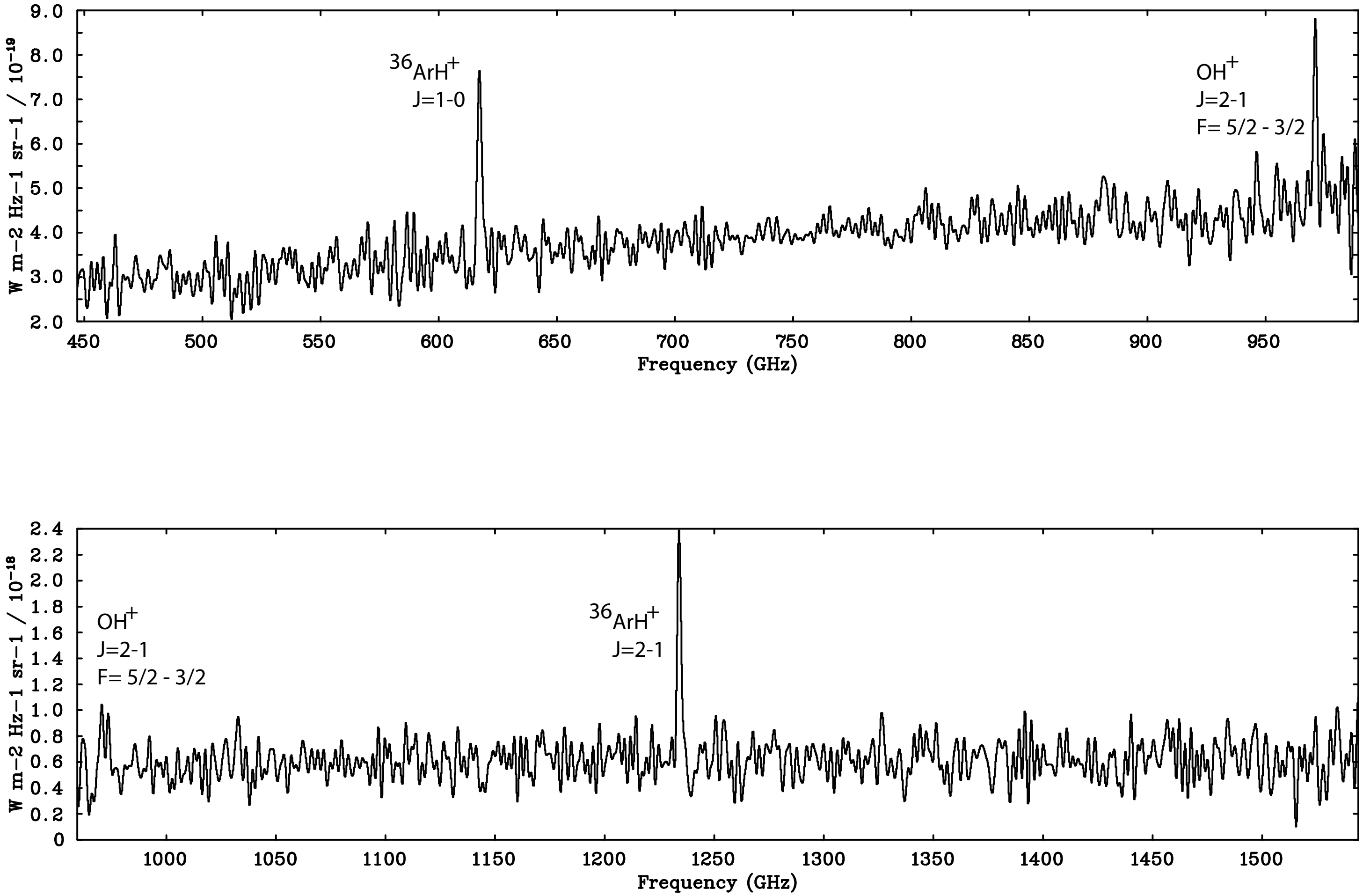

9.0
8.0
7.0
6.0
5.0
4.0
3.0
2.0
W m−2 Hz−1 sr−1 / 10−19
450
500
550
600
650
700
750
800
850
900
950
Frequency (GHz)
36ArH+
J=1-0
OH+
J=2-1
F= 5/2 - 3/2
2.4
2.2
2.0
1.8
1.6
1.4
1.2
1.0
0.8
0.6
0.4
0.2
0
W m−2 Hz−1 sr−1 / 10−18
1000
1050
1100
1150
1200
1250
1300
1350
1400
1450
1500
Frequency (GHz)
OH+
J=2-1
F= 5/2 - 3/2
36ArH+
J=2-1